Modelling of A Helicopter System

K.K.T. Thanapalan
Faculty of Engineering Sciences
University College London
London WC1E 6BT, U.K
E-mail: kary.thanapalan@ucl.ac.uk

***Abstract* — This paper considers modelling and simulation study of a helicopter system – UH-60 Black Hawk helicopter. Mathematical model of single main rotor helicopters is presented in this paper. For the convenience of presentation, force and moment expressions of the various helicopter components are given in the paper to bridge a generic model to the model of UH-60 Black Hawk helicopters. For simulation study a UH-60 like Flightlab GRM model (Generic Rotorcraft Model) is used. Comparisons are made between the simulation results and flight test data. A general agreement exits but where disagreements and anomalies occur, clues are gathered to give explanation. Overall the model represents the UH-60 Black Hawk helicopter. This model can be used for controller development to improve flight handling quality and performances.**

Keywords - modelling; simulation; model validation; helicopter system; flight control

I. Introduction

A helicopter has six degrees of freedom in its motions: up/down, fore/aft (longitudinal motion), left/right (lateral motion), pitching, rolling, and yawing. The motions of a helicopter are achieved by; 1) collectively changing the pitch of all the main rotor blades, thus increasing rotor thrust (collective pitch); 2) cyclically changing the pitch as a sinusoidal function of azimuth which tilts the tip-path-plane fore/aft or left/right and changes the thrust vector direction (cyclic pitch); and 3) collectively changing the tail rotor pitch, which changes tail rotor thrust and thus the yaw moment. A helicopter pilot must simultaneously control three forces and moments, hence, control of a helicopter, is a difficult task indeed. A helicopter pilot typically has at his disposal a cyclic stick to control both fore/aft motions (pitch control) and left/right motion (roll control), a collective lever to control up and down motions (vertical control), and pedals to control left and right yawing motions (yaw control). Lift, thrust, pitching, and rolling control comes from the main rotor while yawing control comes from the tail rotor (Bramwell, 1976, Stepniewski, *et al*, 1984). Analyse the dynamic problems of controlling a helicopter and to develop control schemes for alleviating these problems it is necessary to derive a dynamic model for helicopters. The dynamic model should be well suited to stability and control analysis, which may involve linearized equations of motion about possible equilibrium positions.

In the following section a mathematical model of a single main rotor helicopter is presented. The forces and moments from the different elements of helicopter are discussed in details. Then the model of UH-60 helicopter has been derived and simulation study has been conducted. The results are presented in this paper.

II. Dynamic Model of A Helicopter

The overall vehicle equations of motion are derived. The forces and moments from the different elements of a helicopter, such as main rotor, tail rotor, fuselage and empennage, are discussed in this paper. The helicopter has six degree of freedom in its motion and it has nine state variables in general, which are u, v, w the aircraft velocity components at centre of gravity, p, q, r the aircraft roll, pitch and yaw rates about body reference axes, and θ, ϕ, ψ the Euler angles. To derive the equations of the translational and rotational motions of a helicopter, the helicopter is assumed to be a rigid body referred to an axes system fixed at the centre of mass of the aircraft, so the axes move with time varying velocity components under the action of the applied forces. The Euler angles define the orientation of the fuselage with respect to earth axes system (Padfield, 1996). There are four control inputs, which are, longitudinal cyclic stick (η_{1s}), lateral cyclic stick (η_{1c}) , collective lever (η_c) and pedal input (η_p) which control the helicopter's motion through $X, Y, Z, L, M, and\ N$. So the system equations are as follows

$$\dot{u} = rv - qw - g\sin\theta + X / M_a \tag{1a}$$

$$\dot{v} = pw - ru + g\cos\theta\sin\phi + Y / M_a \tag{1b}$$

$$\dot{w} = qu - pv + g\cos\theta\cos\phi + Z / M_a \tag{1c}$$

$$\dot{p} = \frac{\left(I_{yy} - I_{zz}\right)qr}{I_{xx}} + \frac{I_{xz}\left(pq\left(I_{xx} - I_{yy}\right) + rq + I_{yy} - I_{zz}\right) + I_{xx}^2 pq}{\left(I_{xx}^2 + I_{xx}I_{zz}\right)} + pq + \frac{I_{xz}(N - L)}{\left(I_{xx}^2 + I_{xx}I_{zz}\right)} + L \tag{2a}$$

$$\dot{q} = \frac{1}{I_{yy}}\left[\left(I_{zz} - I_{xx}\right)pr - I_{xz}\left(p^2 - r^2\right)\right] + \frac{1}{I_{yy}}M \tag{2b}$$

$$\dot{r} = \frac{I_{xz}\left(rq - I_{yy} - I_{zz}\right) - I_{xz}^2 pq + pq\left(I_{xx} - I_{yy}\right)}{\left(I_{xz}^2 + I_{xx}I_{zz}\right)} + \frac{N - I_{xz}L}{\left(I_{xz}^2 + I_{xx}I_{zz}\right)} \tag{2c}$$

$$\dot{\phi} = p + q\sin\phi\tan\theta + r\cos\phi\tan\theta \tag{3a}$$

$$\dot{\theta} = q\cos\phi - r\sin\phi \tag{3b}$$

$$\dot{\psi} = q\sin\phi\sec\theta + r\cos\phi\sec\theta \tag{3c}$$

where M_a and g are the mass of the helicopter and acceleration due to gravity, I_{xx}, I_{yy}, I_{zz} are the moment of inertia of the helicopter about x, y and z axes, and I_{xz} the aircraft product of inertia. The model (1) ~ (3) can be considered as a cascade connection nonlinear system, that is, it has the following form:

$$\dot{x} = f_1(x, y) \tag{4}$$

$$\dot{y} = f_2(x,y) + G(y)\ U \tag{5}$$

The overall external forces X, Y and Z along x, y, z axes and moments L, M, N about x, y, z axes can be written as

$$\begin{aligned} X =& \frac{1}{2}\rho(\Omega R)^2 \pi R^2 a_0 s \cos\gamma_s \frac{2C_x}{a_0 s} - \frac{1}{2}\rho(\Omega R)^2 \pi R^2 a_0 s \sin\gamma_s \frac{2C_Z}{a_0 s} \\ &+ \frac{1}{2}\rho(\Omega R)^2 \pi R^2 a_0 s S_P \bar{V}_F^2 C_{XF}(\alpha_F) \end{aligned} \tag{6}$$

$$\begin{aligned} Y =& \frac{1}{2}\rho(\Omega R)^2 \pi R^2 a_0 s\left(\frac{2C_Y}{a_0 s}\right) + \frac{1}{2}\rho(\Omega R)^2 \bar{V}_{FN}^2 S_{FN} C_{YFN}(\beta_{FN}) \\ &+ \frac{1}{2}\rho(\Omega_T R_T)^2 a_{0TT} s_T (\pi R_T)^2 \left(\frac{2C_{TT}}{a_0 s_T}\right) F_T \\ &+ \frac{1}{2}\rho(\Omega R)^2 S_S \bar{V}_F^2 C_{YS} \frac{v_A}{V_F} \end{aligned} \tag{7}$$

$$\begin{aligned} Z =& \frac{1}{2}\rho(\Omega R)^2 \pi R^2 a_0 s\left(\sin\gamma_s\left(\frac{2C_X}{a_0 s}\right) + \cos\gamma_s\left(\frac{2C_Z}{a_0 s}\right)\right) \\ &+ \frac{1}{2}\rho(\Omega R)^2 \bar{V}_T^2 S_{TP} C_{ZTP}(\alpha_{TP}) + S_P \bar{V}_F^2 C_{ZF}(\alpha_F) \end{aligned} \tag{8}$$

and

$$\begin{aligned} L =& \frac{-b}{2} K_\beta \beta_{1s} + h_R\left(\frac{1}{2}\rho\pi R^2 (\Omega R)^2 a_0 s\left(\frac{2C_Y}{a_0 s}\right)\right) \\ &+ h_T . \frac{1}{2}\rho(\Omega_T R_T)^2 a_{0T} s_T (\pi R_T)^2 \left(\frac{2C_{TT}}{a_{0T} s_T}\right) F_T \\ &+ h_{FN} . \frac{1}{2}\rho(\Omega R)^2 \bar{V}_{FN}^2 S_{FN} C_{YFN}(\beta_{FN}) \end{aligned} \tag{9}$$

$$\begin{aligned} M =& \frac{-b}{2} K_\beta \beta_{1s} - h_R . \frac{1}{2}\rho\pi R^2 (\Omega R)^2 a_0 s\left(\cos\gamma_s\left(\frac{2C_x}{a_0 s}\right) - \sin\gamma_s\left(\frac{2C_Z}{a_0 s}\right)\right) \\ &+ x_{cg} . \frac{1}{2}\rho\pi R^2 (\Omega R)^2 a_0 s\left(\sin\gamma_s\left(\frac{2C_x}{a_0 s}\right) + \cos\gamma_s\left(\frac{2C_Z}{a_0 s}\right)\right) \\ &+ (l_{TP} + x_{cg}) \frac{1}{2}\rho(\Omega R)^2 \bar{V}_T^2 S_{TP} C_{ZTP}(\alpha_{TP}) \\ &+ \frac{1}{2}\rho(\Omega R)^2 S_P l_F \bar{V}_F^2 C_{MF}(\alpha_F) \end{aligned} \tag{10}$$

$$\begin{aligned} N =& \frac{1}{2}\rho(\Omega R)^2 \pi R^3 s a_0 \left(\frac{2C_Q}{a_0 s} + \left(\frac{2I_R}{bI_\beta}\right)\frac{\bar{\Omega}'}{\gamma}\right) \\ &- x_{cg}\left(\frac{1}{2}\rho\pi R^2 (\Omega R)^2 a_0 s\left(\frac{2C_Y}{a_0 s}\right)\right) \\ &- (l_T + x_{cg}) \frac{1}{2}\rho(\Omega_T R_T)^2 a_{0T} s_T (\pi R_T)^2 \left(\frac{2C_{TT}}{a_0 s_T}\right) F_T \\ &- (l_{FN} + x_{cg}) \frac{1}{2}(\Omega R)^2 \bar{V}_{FN}^2 S_{FN} C_{YFN}(\beta_{FN}) \\ &+ \frac{1}{2}\rho(\Omega R)^2 S_S l_F \bar{V}_F^2 C_{NF}(\beta_F) \end{aligned} \tag{11}$$

where ρ is air density, R and Ω are the main rotor blade radius and speed, a_0 and s the main rotor blade lift curve slope and solidity, and C_x, C_Y, C_z are the main rotor force coefficients in shaft axes. They are given by

$$\begin{bmatrix} C_X \\ C_Y \end{bmatrix} = \begin{bmatrix} \cos\Psi_w & -\sin\Psi_w \\ \sin\Psi_w & \cos\Psi_w \end{bmatrix} \begin{bmatrix} C_{XW} \\ C_{YW} \end{bmatrix} \tag{12}$$

$$\left(\frac{2C_z}{a_0 s}\right) = -\left(\frac{2C_T}{a_0 s}\right) = -F_0^{(1)} \tag{13}$$

where Ψ_W is the side-slip angle and C_T is the main rotor thrust coefficient given by

$$C_T = \frac{T}{\rho(\Omega R)^2 \pi R^2} \tag{14}$$

The main rotor force coefficients in the hub-wind axes C_{XW} and C_{YW} are can be obtained through equations (15) and (16) in terms of harmonic components of integrated blade aerodynamic loads and harmonics of flapping.

$$\left(\frac{2C_{XW}}{a_0 s}\right) = \left(\frac{F_0^{(1)}}{2} + \frac{F_{2c}^{(1)}}{4}\right)\beta_{1cw} + \frac{F_{1c}^{(1)}}{2}\beta_0 + \frac{F_{2s}^{(1)}}{4}\beta_{1sw} + \frac{F_{1s}^{(2)}}{2} \tag{15}$$

$$\left(\frac{2C_{YW}}{a_0 s}\right) = \left(\frac{F_0^{(1)}}{2} + \frac{F_{2c}^{(1)}}{4}\right)\beta_{1sw} - \frac{F_{1s}^{(1)}}{2}\beta_0 - \frac{F_{2s}^{(1)}}{4}\beta_{1cw} + \frac{F_{1c}^{(2)}}{2} \tag{16}$$

where β_0 is the coning angle and β_{1cw}, β_{1sw} are the first harmonic cyclic flapping angles. The harmonic components of integrated blade aerodynamic loads are given by the following expressions

$$F_0^{(1)} = \theta_0\left(\frac{1}{3} + \frac{\mu^2}{2}\right) + \frac{\mu}{2}\left(\theta_{1sw} + \frac{\bar{p}_w}{2}\right) + \left(\frac{\mu_z - \lambda_0}{2}\right) + \frac{1}{4}(1 + \mu^2)\theta_{tw} \tag{17}$$

$$F_{1s}^{(1)} = \frac{\alpha_{sw} + \theta_{1sw}}{3} + \mu\left(\theta_0 + \mu_z - \lambda_0 + \frac{2}{3}\theta_{tw}\right) \tag{18}$$

$$F_{1c}^{(1)} = \frac{\alpha_{cw} + \theta_{cw}}{3} - \frac{\mu\beta_0}{2} \tag{19}$$

$$F_{2s}^{(1)} = \frac{\mu}{2}\left\{\theta_{1cw} - \beta_{1sw} + \frac{\bar{q}_w - \lambda_{1cw}}{2} - \mu\beta_0\right\} \tag{20}$$

$$F_{2c}^{(1)} = -\frac{\mu}{2}\left\{\theta_{1sw} + \beta_{1cw} + \frac{\bar{p}_w - \lambda_{1sw}}{2} + \mu\left(\theta_0 + \frac{\theta_{tw}}{2}\right)\right\} \tag{21}$$

$$\begin{aligned} F_{1s}^{(2)} =& \frac{\mu^2}{2}\beta_0\beta_{1sw} + \left(\mu_z - \lambda_0 - \frac{\mu}{4}\beta_{1cw}\right)_{\alpha_{sw}} - \frac{\mu}{4}\beta_{1sw}\alpha_{cw} \\ &+ \theta_0\left(\frac{\alpha_{sw}}{3} + \mu(\mu_z - \lambda_0) - \frac{\mu^2}{4}\beta_{1cw}\right) + \left(\frac{\alpha_{sw}}{4} + \frac{\mu}{2}\left(\mu_z - \lambda_0 - \frac{\beta_{1c}\mu}{4}\right)\right)\theta_{tw} \\ &+ \theta_{1sw}\left(\frac{\mu_z - \lambda_0}{2} + \mu\left(\frac{3}{8}(\bar{p}_w - \lambda_{1sw}) + \frac{\beta_{1cw}}{4}\right)\right) \\ &+ \frac{\mu}{4}\theta_{1cw}\left(\frac{\bar{q}_w - \lambda_{1cw}}{2} - \beta_{1sw} - \mu\beta_0\right) - \frac{\delta\mu}{a_0} \end{aligned} \tag{22}$$

$$
\begin{aligned}
F_{1c}^{(2)} &= -2\beta_0\mu\left(\mu_z-\lambda_0-\frac{4}{3}\mu\beta_{1cw}\right)+\left(\mu_z-\lambda_0-\frac{3}{4}\beta_{1cw}\mu\right)\alpha_{cw} \\
&-\frac{\mu}{4}\beta_{1sw}\alpha_{sw}+\theta_0\left(\frac{\alpha_{cw}}{3}-\frac{\mu}{2}\left(\beta_0+\frac{\mu}{2}\beta_{1sw}\right)\right)+\theta_{tw}\left(\frac{\alpha_{cw}}{4}-\mu\left(\frac{\beta_0}{3}+\frac{\mu}{8}\beta_{1sw}\right)\right) \\
&+\theta_{1cw}\left(\frac{\mu_z-\lambda_0}{2}+\frac{\mu}{4}\left(\frac{\bar{p}_w-\lambda_{1sw}}{2}-\beta_{1cw}\right)\right) \\
&+\frac{\mu}{4}\theta_{1sw}\left(\frac{\bar{q}_w-\lambda_{1cw}}{2}-\beta_{1sw}-\mu\beta_0\right)
\end{aligned} \tag{23}
$$

where θ_0 is the main rotor collective pitch and is given by

$$
\theta_0 = \frac{(g_{c0}+g_{c1}\eta_c)+(k_g\Delta n)}{1+\tau_{c4}s} \tag{24}
$$

In equation (24), g_{c0} and g_{c1} are the collective gearing constants, k_g and Δn the autostabiliser feed back gain and aircraft normal acceleration increment, and η_c the collective lever variable (control input).

$\theta_{1cw}, \theta_{1sw}$ blade cyclic pitch components in hub-wind axes are defined by

$$
\begin{bmatrix} \theta_{1sw} \\ \theta_{1cw} \end{bmatrix} = \begin{bmatrix} \cos\Psi_w & \sin\Psi_w \\ -\sin\Psi_w & \cos\Psi_w \end{bmatrix} \begin{bmatrix} \theta_{1s} \\ \theta_{1c} \end{bmatrix}, \tag{25}
$$

where θ_{1s}, θ_{1c} are the longitudinal and lateral cyclic pitch they are determined by

$$
\begin{aligned}
\theta_{1s} &= \left[\frac{g_{1s0}+g_{1s1}\eta_{1s}+g_{sc0}+g_{sc1}\eta_c+k_\theta\theta+k_q q+k_{1s}(\eta_{1s}-\eta_{1s0})}{1+\tau_{c1}s}\right]\cos\psi_F \\
&+\left[\frac{g_{1c0}+g_{1c1}\eta_{1c}+k_\phi\phi+k_P P+k_{1c}(\eta_{1c}-\eta_{1c0})}{1+\tau_{c2}s}\right]\sin\psi_F
\end{aligned} \tag{26}
$$

$$
\begin{aligned}
\theta_{1c} &= \left[\frac{g_{1c0}+g_{1c1}\eta_{1c}+k_\phi\phi+k_P P+k_{1c}(\eta_{1c}-\eta_{1c0})}{1+\tau_{c2}s}\right]\cos\psi_F \\
&-\left[\frac{g_{1s0}+g_{1s1}\eta_{1s}+g_{sc0}+g_{sc1}\eta_c+k_\theta\theta+k_q q+k_{1s}(\eta_{1s}-\eta_{1s0})}{1+\tau_{c1}s}\right]\sin\psi_F
\end{aligned} \quad , \tag{27}
$$

where k_ϕ, k_p, k_θ *and* k_q feedback gains, k_{1c} *and* k_{1s} are feed forward gains. η_{1s0}, *and* η_{1c0} are constants, adjustable by the pilot and η_{1c}, η_{1s} are lateral and longitudinal cyclic stick variables (control inputs).

The tail rotor provides control for the *yaw*, whose only responsibility is to provide a sideways thrust force and thereby produce a yawing moment about the main rotor shaft (Newman, 1994, Leishman, 2000) i.e. contributes the external force Y, moments L, and M (see equations (7), (9) and (11)). Tail rotor contributaion can be determined by

$$
\left(\frac{2C_{TT}}{a_{0T}s_T}\right) = \frac{1}{3}.\frac{\theta_{0T}+K_3\left(\frac{n_\beta}{\lambda_\beta^2}\right)_T\frac{4}{3}(\mu_{zT}-\lambda_{0T})}{1-K_3\left(\frac{n_\beta}{\lambda_\beta^2}\right)_T(1+\mu_T^2)}.\left(1+\frac{3}{2}\mu_T^2\right)+\left(\frac{\mu_{zT}-\lambda_{0T}}{2}\right), \tag{28}
$$

where θ_{0T} is a tail rotor pitch (control input) and is given by

$$
\theta_{0T} = \frac{g_{t0}+g_{t1}\left(g_{ct0}(1-\eta_P)+(1-2g_{ct0})\eta_C\right)+k_\psi(\psi-\psi_H)+k_r r}{1+\tau_{c3}s} \tag{29}
$$

In equation (29), g_{t0}, g_{t1} are pedals gearing constants, and g_{ct0} is the pedal cable gearing constant. η_c, η_p are the collective liver variable and pedal variable, which are the control inputs.

Almost all of the performance characteristics of a helicopter depend on the power-plant performance (Prouty, 1986). Here a simplified model for a helicopter rotor-speed, associated engine and rotor governor dynamics formulae are presented as follows.

$$
\dot{\Omega} = \frac{1}{I_R}(Q_E-Q_R-G_TQ_T)+\dot{r} \tag{30}
$$

$$
Q_E = -K_3(\Omega-\Omega_i) \tag{31}
$$

$$
Q_R = \frac{1}{2}\rho(\Omega R)^2\pi R^3 s a_0\left(\frac{2C_Q}{a_0 s}\right) \tag{32}
$$

$$
Q_T = \frac{1}{2}\rho(\Omega_T R_T)^2\pi R_T^3 s_T a_{0T}\left(\frac{2C_{QT}}{a_{0T}s_T}\right) \tag{33}
$$

In time domain, differential equation can be written as

$$
\ddot{Q}_E = \frac{1}{\tau_{e1}\tau_{e3}}\left\{-(\tau_{e1}+\tau_{e3})\dot{Q}_E-Q_E+K_3\left(\Omega-\Omega_i+\tau_{e2}\dot{\Omega}\right)\right\} \tag{34}
$$

where Q_E, Q_R and Q_T are the engine, main rotor, and tail rotor torques, respectively. G_T is the tail rotor gear ratio. I_R is the moment of inertia of the rotating system. Ω_i is the idling rotor speed and K_3 overall engine/rotor speed gain.

Some assumptions are made to produce a closed form of expressions to the helicopter motion, which are shown below. The tail rotor flapping is ignored. For the main rotor, flapping angles are assumed small and the overall fuselage acceleration and blade weight effects are neglected. Yaw rate and sideslip rate, are assumed small compared with rotor angular rate Ω in the kinematics of blade motion. Especially, basic assumptions regarding to the rotor blade aerodynamics are summarised as follows:

- A constant, two-dimensional, lift curve slope is assumed.
- Compressibility effects are ignored.
- Stall and reversed flow effects are ignored.
- The induced velocity distribution, normal to the rotor disc, includes linear longitudinal and lateral variations, the value at the centre satisfying simple momentum considerations.
- Couplings from blade pitch and lag dynamics into flapping motion are ignored.
- Quasi-steady flapping and coning are used in the derivation of the reaction forces and moments on the fuselage, i.e., the interaction of disc tilt modes with fuselage mode are neglected.

These assumptions make it possible to integrate the aerodynamic loading analytically and hence produce the closed form of expressions for the rotor forces and moments.

III. SIMULATION STUDY OF UH-60 BLACK HAWK HELICOPTER USING FLIGHTLAB

A similar approach has been taken for modelling main rotor and tail rotor apart from that the tail rotor flapping has been ignored. In Flightlab, the tail rotor component implemented is based on a simplified theoretical method of determining the characteristics of a lifting rotor in forward flight (report No 716 National Advisory committee for Aeronautics by F.J. Bailey, Jr,) which is called bailey rotor. The co-ordinate system of the bailey rotor has X forward into the free-stream airflow and Z in the direction of thrust. Rotor thrust and torque are calculated as functions of the blade tip loss factor by making the similar assumptions as mentioned above. Bailey derived rotor thrust and torque by analytically integrating the air-loads over the rotor blade span and averaging them over the azimuth. For the bailey rotor, using a reasonable initial value for the tail rotor thrust T_T , the thrust coefficient C_{TT} can be calculated from momentum theory as

$$C_{TT} = \frac{T_T}{\rho(\Omega_T R_T)^2 \pi R_T^2 k_{bl}} \tag{35}$$

The only difference from mathematical model described in (28) is that the blockage effect, k_{bl} , is introduced due to fin consideration. Total inflow λ_0 and the induced velocity v_i can be calculated by

$$\lambda_0 = \frac{-\mu_z + \frac{1}{2}C_{TT}}{\sqrt{\left(\mu^2 + \frac{1}{2}C_{TT}\right)}} \tag{36}$$

$$v_i = \mu_z - \lambda_0 \tag{37}$$

Using these values, an iterative procedure is performed to determine the values of the total inflow. This is done by using the equation below derived by applying momentum theory.

$$v_i = \frac{a_{0T} s_T}{2}\left[\frac{\mu_z t_{3,1} + \theta_0 t_{3,2} + \theta_1 t_{3,3}}{2\sqrt{\left(\mu^2 + \lambda_0^2\right)} + \frac{a_{0T} s_T}{2} t_{3,1}}\right] \tag{38}$$

where θ_0 and θ_1 are the blade collective pitch at the root and tip, respectively. λ_0 is the total inflow across the rotor disk. The values $t_{3,1}$, $t_{3,2}$ and $t_{3,3}$ are computed by

$$t_{3,1} = \frac{1}{2}B^2 + \frac{1}{4}\mu^2 \tag{39}$$

$$t_{3,2} = \frac{1}{2}B^3 + \frac{1}{2}B\mu^2 \tag{40}$$

$$t_{3,3} = \frac{1}{4}B^4 + \frac{1}{4}B^2\mu^2 \tag{41}$$

Once the values of $t_{3,1}$, $t_{3,2}$ and $t_{3,3}$ have been determined within a reasonable tolerance, the induced velocity is again calculated using the above equation. From equation (36) the thrust coefficient is then recalculated using

$$C_{TT} = 2v_i\sqrt{\left(\mu^2\lambda_0^2\right)} \tag{42}$$

The rotor thrust can then be calculated with the following equation:

$$T_T = \frac{\pi}{180}\rho k_{bl}\pi\left(\Omega_T R_T^2\right)^2, \tag{43}$$

where the blockage effect, k_{bl} , due to a fin is used to modify the rotor thrust as a function of the velocity which is given by,

$$k_{bl} = (1 - b_{t1})\frac{u_A^2}{v_{bl}^2} + b_{t1}, \quad \{u_A \le v_{bl}\} \tag{44}$$

$$k_{bl} = b_{t2}, \quad \{u_A \ge v_{bl}\} \tag{45}$$

in equations (44) and (45) the transition velocity, v_{bl} and the tail blockage constants, b_{t1} and b_{t2} , are specified by the users. This allows calculating the root collective pitch θ_0 by

$$\theta_0 = \frac{\pi}{180}\left[-T_T\delta_3 \tan\delta_3\right] + \theta_{bias} + \theta_c , \tag{46}$$

where θ_c is the commanded root collective pitch, θ_{bias} is a preset collective pitch bias, T_T is the tail rotor thrust, and δ_3 is the hinge skew angle for pitch-flap coupling. In addition, for the main rotor, in Flightlab model, aerodynamic effect has been taken into account. In more details, the aerodynamic components are numeric components that allow the computation of airloads, inflow, and interference. Airloads are computed to give the motion of the attached structural component and inflow is computed based on the airloads. Additionally, interference between the aerodynamic components can be computed.

Fuselage and empennage components are implemented in Flightlab model, by using simple aerodynamics laws, in which the forces and moments from these elements are given by functions of incident and sideslip angle. In the process of modelling due to the complex flow field around helicopter fuselages and the interaction of the main rotor wake with the fuselage, some difficulties are caused to construct the forces and moments equations. So the direct results from wind tunnel test data gathered from various sources are used (Biggers, 1962, Wilson, *et at*, 1975). The engine output torque is controlled by the governor system that senses a change in rotor speed Ω and demands a fuel flow change ω_f . The fuel change is represented as a single lag.

$$\tau_{e1}\dot{\omega}_f + \omega_f = K_{e1}\Delta\Omega , \tag{47}$$

where τ_{e1} and K_{e1} are the time constant and gain respectively. K_{e1} is the slope of the droop in the rotor speed from flight idle to maximum contingency fuel flow.

$$\Delta\Omega = \Omega - \Omega_i , \tag{48}$$

where $\Delta\Omega$ and Ω_i are the changes in rotor speed and flight idle rotor speed, respectively. The engine torque Q_E response to the fuel flow change is described by a lag responding to fuel flow and flow rate

$$\tau_{e3}\dot{Q}_E + Q_E = K_{e2}\left(\tau_{e2}\dot{\omega}_f + \omega_f\right) \quad , \tag{49}$$

where K_{e2} is the gain and τ_{e2} , τ_{e3} are the time constants. Combining the above results gives a second order ordinary differential equation as follows

$$\ddot{Q}_E = \frac{1}{\tau_{e1}\tau_{e3}}\left\{-\left(\tau_{e1}+\tau_{e3}\right)\dot{Q}_E - Q_E + K_3\left(\Omega - \Omega_i + \tau_2\dot{\Omega}\right)\right\} \tag{50}$$

The equation is further normalised by maximum engine torque $Q_{E\max}$ as

$$\left(\tau_{e1}\tau_{e3}\right)\ddot{\overline{Q}}_E + \left(\tau_{e1}+\tau_{e3}\right)\dot{\overline{Q}}_E + \overline{Q}_E = \frac{K_3}{Q_{E\max}}\left[\left(\Omega - \Omega_i\right) + \tau_{e2}\dot{\Omega}\right] \tag{51}$$

Where $\overline{Q}_E = \dfrac{Q_E}{Q_{E\max}} K_3 = K_{e1}K_{e2}$ (52)

With $K_3 = -\dfrac{Q_{E\max}}{\Omega_i\left(1 - \dfrac{\Omega_m}{\Omega_i}\right)}$ (53)

Ω_m is the rotor speed at maximum contingency fuel flow. Similarly in the mathematical model the simplified free turbine engine equations are also presented (see equation (34)).

In the flight control system, essentially, signals from the cyclic stick, collective lever and yaw pedals are transmitted to the main and tail rotor blades. Inter-links between collective lever, main rotor cyclic, and tail rotor collective pitch are also incorporated in the mathematical model. These pilot generated signals are combined with error signals from the stabilisation and automatic flight control systems and passed through a first order lag. The autostabiliser transmits signals from rate and attitude gyros to produce feedback control of roll through lateral cyclic, pitch through longitudinal cyclic and yaw through tail rotor collective. Feed forward signals are also incorporated in the cyclic loops for compensation also normal acceleration is fed back into the main rotor collective channel to reduce adverse rotor pitching moments at high forward speeds. In Flightlab model the control components are designed as multi input/ mulit output, linear and nonlinear sub system.

Simulation results are presented in this paper. The appropriate parameters for the UH-60 helicopters are used in the simulation studies are presented in the appendix Table A.1~A.4. Comparison result shows that there is a general agreement between the flight test data and the Flightlab GRM model simulation results. The flight test data were generated from the tests conducted for the UH-60 helicopter under very calm wind condition at Navy crows landing, California in September 1992 (Fletcher, 1993, Fletcher, 1995).

Simulation with two dynamics manoeuvres (Hover and 80Kts) for the four control input has been carried out. The model response was computed using the actual flight measured control positions. Both the flight data and the simulation data ware plotted in the same scale, which enables an easier comparison of the variables of interest, such as translational velocities (u, v, w), rotational velocities $(p, q\ ,\ r\ )$, Euler angles (ϕ, θ, ψ) and body axes accelerations (a_x, a_y, a_z) . In this paper longitudinal stick input simulation results are choosen as an example, which are shown In Fig. 3.1(a) and Fig. 3.1(b). The pilot's longitudinal stick input was used to drive the model in hover condition and 80Kts forward flight speed.

There exists reasonably good correlation with the flight data response, however some discrepancies are evident in the pitch rate (q) . Initially it starts with a good agreement but tends to differ in the long term, which might be an indication of that some unstable factors in real flight vehicle have not been included into the mathematical model.

IV. CONCLUDING REMARKS

The paper describes modelling and simulation study of a helicopter system. The mathematical model for a helicopter has been developed for simulation study and control analysis.
For the simulation study in the paper a UH-60 like Fightlab GRM model has been used. The model responses are compared with UH-60 flight test data in both hover and 80Kts forward flight conditions. Correlation in the main is satisfactory but anomalies are present. The possible reasons for those anomalies are suggested. Overall satisfactory results are achieved. Simulation analyses with the mathematical model itself are currently undergoing and the results will be investigated for the analysis of the system stability and control.

REFERENCES

[1] Biggers, J.C., McCloud, J.L., and Patterakis, P., Wind tunnel tests on two full scales helicopter fuselage, NASA TN-D-154-8, 1962.

[2] Bramwell, A.R.S., Helicopter Dynamics, Edward Arnold 1976

[3] Fletcher, J.W., Identification of UH-60 stability derivative models in hover from flight test data, AHS, May 1993.

[4] Fletcher, J.W., A model structure for identification of linear models of the UH-60 helicopter in hover and forward flight, NASA TM 110362, August 1995

[5] Hilbert, K.B., A Mathematical Model of the UH-60 Helicopter, NASA TM-85890, 1984.

[6] Leishman, G., The Principles of Helicopter Aerodynamics, Cambridge University Press 2000.

[7] Newman, S., The Foundations of Helicopter Flight, Arnold, A member of the Hodder Headline Group, London 1994

[8] Padfield, G.D., "Helicopter Dynamics and Flight Control, Blackwell Science Ltd., 1996.

[9] Prouty, R., Helicopter Performance, Stability and Control, PWS Publishers, 1986.

[10] W.Z. Stepniewski and C.N. Keys, "Rotary-Wing Aerodynamics", Dover Publications, Inc, New York, Vol. 2, 1984.

[11] J.C. Wilson and R.E. Mineck, "Wind Tunnel investigation of helicopter – Rotor wake effects on three helicopter fuselage model", NASA TM-X-3185, 1975

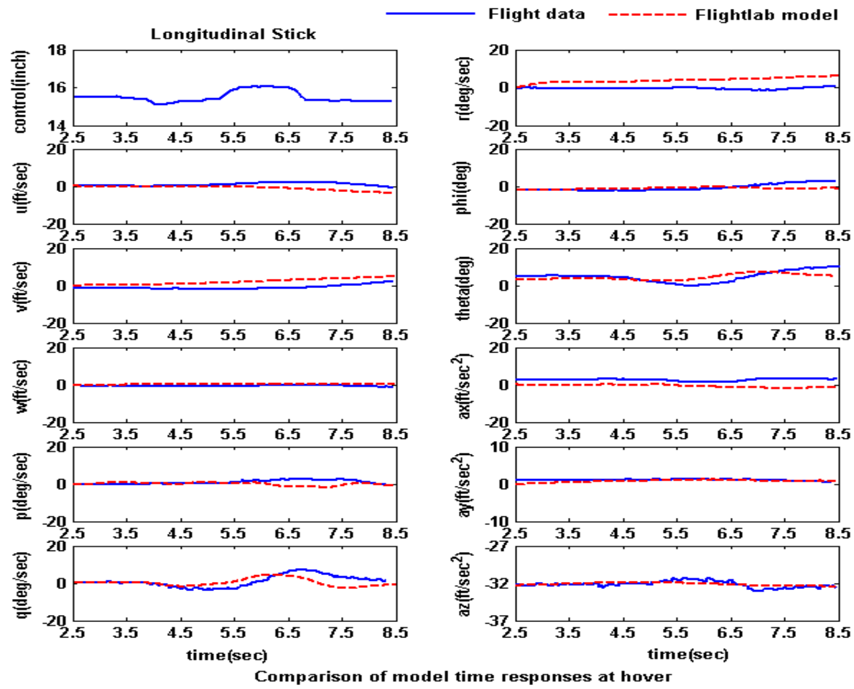

Figure. 3.1(a) Comparison of helicopter dynamic responses at hover between flight test data and FGR model for longitudinal stick input

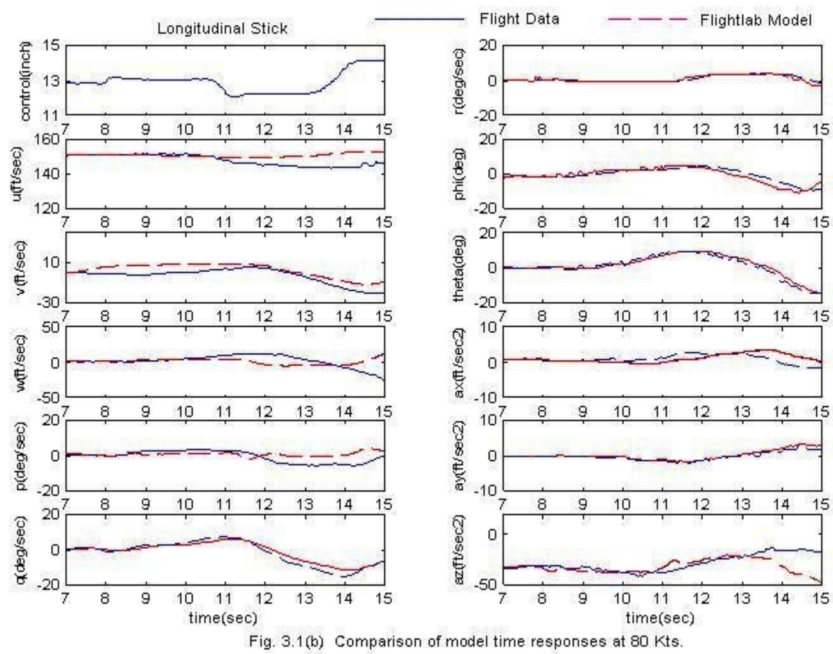

Figure. 3.1(b) Comparison of helicopter dynamic responses at 80Kts between flight test data and FGR model for longitudinal stick input

APPENDIX A

PARAMETER OF UH-60 HELICOPTER

UH-60 helicopter data are gathered from various sources are presented below (eg. Hilbert, 1984).

Table A.1 Aircraft mass and inertia:

Description	Symbol	UH-60 value	Units
mass of the helicopter	M_a	15350	lb
aircraft roll inertia	I_{xx}	5629	$slug\ ft^2$
aircraft pitch inertia	I_{yy}	40000	$slug\ ft^2$
aircraft yaw inertia	I_{zz}	37200	$slug\ ft^2$
aircraft product of inertia	I_{xz}	1670	$slug\ ft^2$
centre of gravity location	-	(36.0 0 4.7)	ft
Fuselage reference pt.	-	(34.6 0 23.4)	ft

Table A.2 Main rotor group:

Description	Symbol	UH-60 value	Units
main rotor speed	Ω	27.0	$rad/\sec$
main rotor blade radius	R	26.83	ft
blade lift curve slope	a_0	5.73	rad^{-1}
main rotor solidity	s	0.08210	-
rotor shaft forward tilt	γ_s	0.05236	rad
rotor thrust coefficient	C_T	0.1846	-
number of blades	b	4	-
blade lock number	$\gamma(\gamma_0)$	8.1936	-
rotor inertia number	η_β	1.0242	-
flap frequency ratio	λ_β	1	-
linear blade twist	θ_{tw}	-0.3142	rad
Z co-ordinate of rotor hub	h_R	31.5	ft
mixing angle	ψ_F	0.175	rad
blade chord	c	1.73	ft
flapping spring const.	K_β	0	-
c.g. location fwd.of fuselage ref. Point	x_{cg}	1.4	ft
Stiffness number	S_β	0	-
blade profile drag coefficient	δ_0	-0.0216	-
air density	ρ	0.002473	$slug/ft^3$
blade flapping moment of inertia	I_β	3.10	$slug\ ft^2$

Table A.3 Empennage:

Description	Symbol	UH-60 value	Units
tail plane area	S_{TP}	45.0	ft
lift curve slope at zero incident	a_{0TP}	4	-
Location aft of fuselage reference point	l_{TP} , l_{FN}	70.0	ft
fin area	S_{FN}	32.3	ft^2

Table A.4 Tail rotor group:

Description	Symbol	UH-60 value	Units
tail rotor blade radius	R_T	5.5	ft
tail rotor speed	Ω_T	124.62	rad/s
blade lift curve slope	a_{0T}	5.73	rad^{-1}
tail rotor solidity	s_T	0.1875	-
fin blockage factor	F_T	-0.402	-
tail rotor inertia number	$(n_\beta)_T$	0.4223	-
flap frequency ratio	$(\lambda_\beta)_T$	1.0	-
tail rotor location aft of fuselage reference point	l_T	73.2	ft
Negative z co-ordinate of hub	h_T	32.5	ft
linear blade twist	θ_{tw}	-18.0	deg
Number of rotor blade	b	4	-
blade profile drag coefficient	δ_{0T}	-0.0216	-
blade lift dependent drag coefficient	δ_{2T}	0.40	-
pitch/flap coupling (δ_3)	k_3	0.700	-
blade lock number	$(\gamma)_T$	3.378	-